

# Vibrational Spectra and Conformations of Cyanocyclobutane

D. L. Powell,<sup>a,b</sup> A. Gatial,<sup>a</sup> P. Klæboe,<sup>a,\*</sup> C. J. Nielsen,<sup>a</sup> A. J. Kondow,<sup>b</sup> W. A. Boettner<sup>b</sup> and A. M. Mulichak<sup>b</sup>

<sup>a</sup>Department of Chemistry, University of Oslo, Box 1033, N-0315 Oslo 3, Norway and <sup>b</sup>Department of Chemistry, The College of Wooster, Wooster, OH 44091, USA

Powell, D. L., Gatial, A., Klæboe, P., Nielsen, C. J., Kondow, A. J., Boettner, W. A. and Mulichak, A. M., 1989. Vibrational Spectra and Conformations of Cyanocyclobutane. – *Acta Chem. Scand.* 43: 441–449.

The IR and Raman spectra of cyanocyclobutane as a vapour, liquid and as amorphous and crystalline solids were recorded at various temperatures. High pressure IR spectra of the liquid and crystalline phases were recorded at ca. 20 kbar pressure. IR matrix isolation spectra in argon and nitrogen matrices were recorded at 14 K, using the hot-nozzle technique.

The spectra are interpreted in terms of a dominant equatorial conformer and an axial conformer which is present under ordinary conditions in less than 10 % abundance. However, in spite of its low concentration, it appears to be the axial conformer which crystallizes at high pressure. The enthalpy difference between the conformers was determined to  $4.8 \pm 0.4 \text{ kJ mol}^{-1}$  in the liquid, and the barrier to ring conversion was less than  $5 \text{ kJ mol}^{-1}$  from the axial conformer. A vibrational assignment is made, supported by normal coordinate calculations.

We have been interested in the conformational equilibria in cyclobutanes for several years. As is well known, most cyclobutanes are non-planar.<sup>1</sup> Each substituent can be described as axial or equatorial in a way analogous to that used in the more thoroughly studied cyclohexanes. Unlike the cyclohexanes, though, the equilibria in cyclobutanes lie much more to one side (that in which the substituent is equatorial), so far in fact that it has been difficult to isolate or provide firm evidence for a second, axial, conformer. We recently reported our work on chlorocyclobutane and bromocyclobutane,<sup>2</sup> at which time we also gave a more general background to the problem. The very recent results on methylcyclobutane<sup>3</sup> should be noted as demonstrating a case in which the equilibrium is not quite so one-sided. We now wish to report our rather surprising results in the same quest for cyanocyclobutane (CYCB).

Although no complete vibrational study has been performed for CYCB except for a Raman study of the liquid many years ago,<sup>4</sup> the far infrared spectrum of its ring puckering mode was interpreted<sup>5</sup> in terms of a potential function which is “totally devoid of a second minimum”. In two independent microwave studies in each of which the possibility of an axial conformer was considered, no evidence for one was found.<sup>6,7</sup> In the latter paper<sup>7</sup> the authors felt that their inability to identify lines belonging to a second conformer indicated that any second minimum in the potential function must be at least  $350 \text{ cm}^{-1}$  (ca.  $4 \text{ kJ mol}^{-1}$ ) above the ground state.

Quite recently, with the assistance of *ab initio* calculations, the microwave spectrum of the axial conformer was obtained and interpreted.<sup>8</sup> With that in hand, several vibra-

tional satellites for both conformers were assigned, leading to the result that the ground states of the two conformers are approximately  $3 \text{ kJ mol}^{-1}$  apart in the vapour.<sup>9</sup>

## Experimental

CYCB was obtained from a variety of commercial sources. The samples used were checked by gas chromatography and had no detectable impurities.

Infrared spectra were recorded on a Perkin-Elmer model 283 spectrometer, a Perkin-Elmer model 225 spectrometer, and a Bruker IFS-114c evacuable Fourier transform spectrometer. Spectra were taken of the compound as a vapour, as a liquid and as unannealed and annealed solids at both low temperature and high pressure. For the high-pressure spectra a diamond-anvil cell from High Pressure Diamond Optics and a Perkin-Elmer  $4 \times$  beam condenser were employed.

Spectra were also recorded of the compound isolated in argon and nitrogen matrices on a CsI window in a Displex unit from Air Products. Using a heated quartz nozzle, the sample was deposited not only from a 1000:1 mixture of gas at room temperature, but also at temperatures up to 900 K. The temperature of the window was 17 K during deposition and 13 K during recording of spectra. No decomposition products were detected at any time.

Raman spectra were recorded of the liquid and the annealed crystalline solid as well as of the liquid at different temperatures in a capillary tube of 2 mm inner diameter surrounded by a Dewar and cooled by gaseous nitrogen. These measurements were made using a Dilor RT 35 spectrometer (triple monochromator) interfaced to the Aspect 2000 data system of the Bruker FTIR and excited by the

\* To whom correspondence should be addressed.

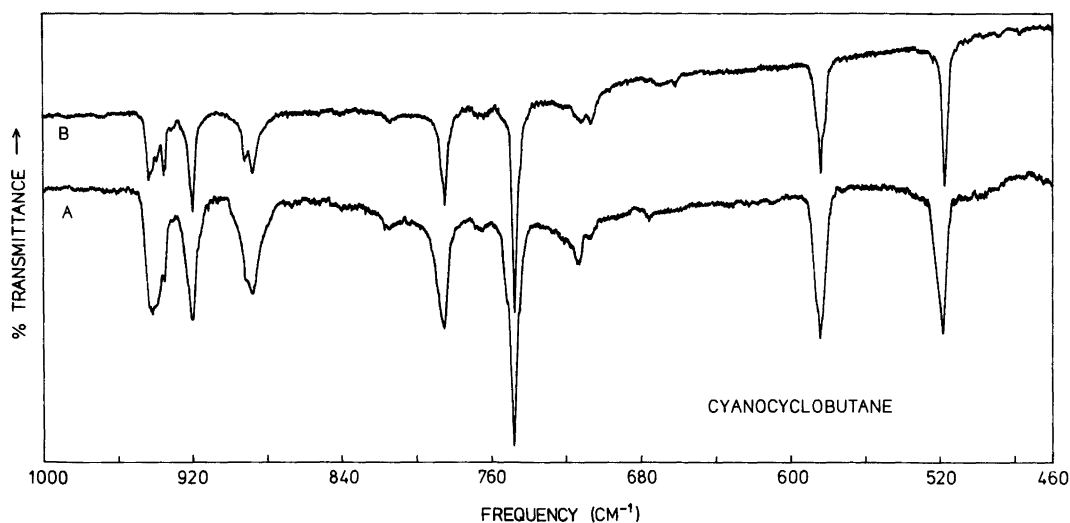


Fig. 1. Infrared (IR) spectral curves for cyanocyclobutane (CYCB) matrix isolated in nitrogen (1:700) at 14 K; curve B, nozzle temperature 312 K; curve A, nozzle temperature 900 K.

514.8 nm line of a Spectra Physics model 2000 argon ion laser.

### Results and discussion

The experimental results obtained are presented in Table 1. Portions of the IR spectra in a nitrogen matrix generated with deposition temperatures of 300 and 900 K are given in Fig. 1. Mid IR spectra of the low-temperature crystal and high-pressure crystal are given in Figs. 2 and 3, respectively. The Raman spectrum of CYCB as a liquid is given in Fig. 4 and that of the low-temperature crystal in Fig. 5. Portions of the Raman spectra of the liquid at various temperatures are shown in Figs. 6 and 7.

*Vapour and liquid spectra.* Since the vapour pressure of CYCB is low at ambient temperature, the IR vapour spectrum, recorded in a cell of 1 m path, was incomplete and no Raman vapour spectrum was obtained.

The IR and Raman spectra of the liquid were carefully recorded. The weak IR and Raman bands recorded in the liquid state, which are discussed below, are essential to understand the conformations of CYCB. As for chloro- and bromocyclobutane,<sup>2</sup> the low barrier to ring inversion<sup>8,9</sup> in CYCB prevented the high-energy conformer (axial) from being isolated in the matrix at 17 K or in the amorphous solid at 85 K (see below). In the vapour and liquid at ambient (and higher) temperatures the axial conformer can be observed.

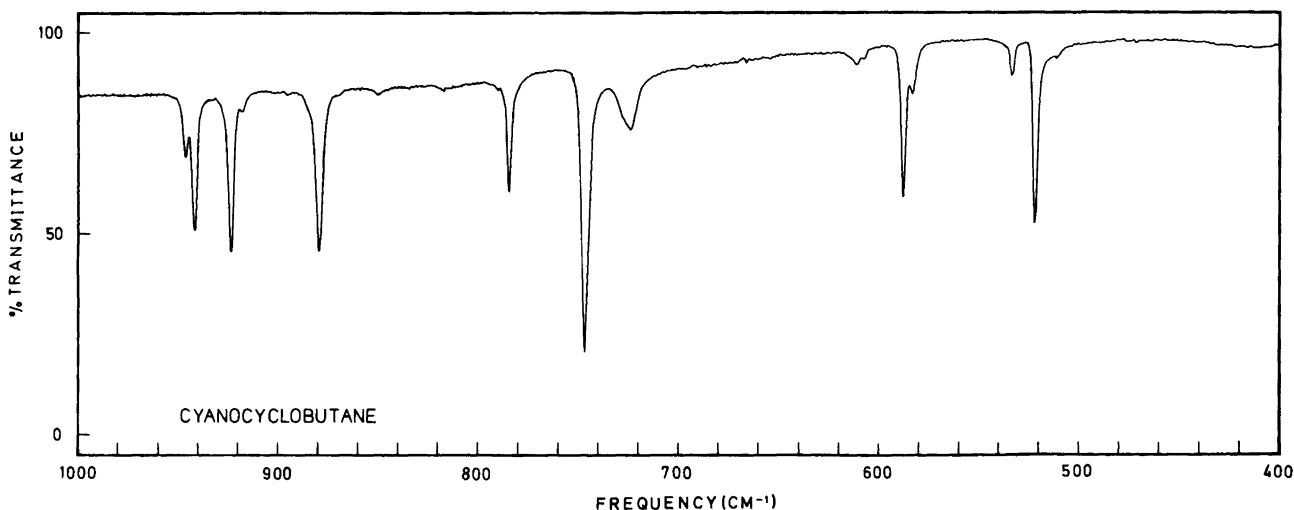


Fig. 2. An IR spectrum of CYCB as a crystalline solid (crystal III, see text) at 85 K, formed by annealing an amorphous solid at 185 K.

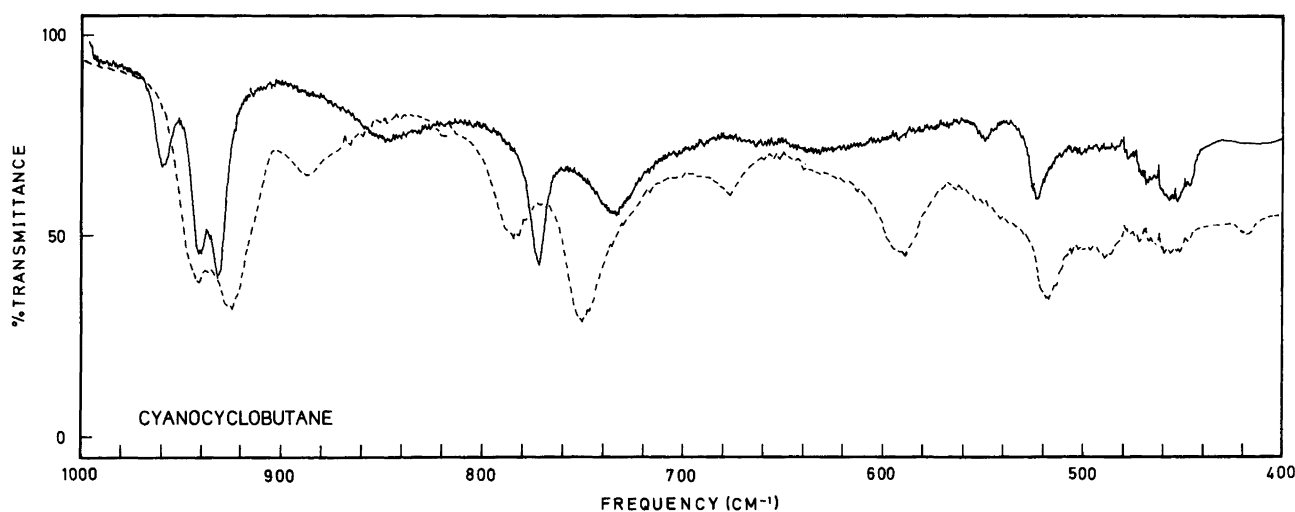


Fig. 3. IR spectra of CYCB as a liquid (dashed curve) and as a high-pressure crystal (same sample) at 20 kbar (solid curve) in a diamond-anvil cell.

The Raman spectrum of liquid CYCB was recorded at a number of temperatures ranging from 379 K to 202 K with two purposes in mind: (a) to observe the band intensity variations with temperature and calculate the  $\Delta H^0$  (axial-equatorial); (b) the Raman bands become sharper at lower temperatures and overlapping bands, including polarization ratios, can be more accurately studied.

From these measurements it was clear that the Raman bands at 1025, 865, 676 and 486  $\text{cm}^{-1}$  (axial) were enhanced at higher temperatures relative to the neighbour bands at 1049, 885, 587 and 521  $\text{cm}^{-1}$  (equatorial). From the intensity variations of the band pairs, the  $\Delta H^0$  (axial-equatorial) of the liquid was determined as  $4.8 \pm 0.4 \text{ kJ mol}^{-1}$ .

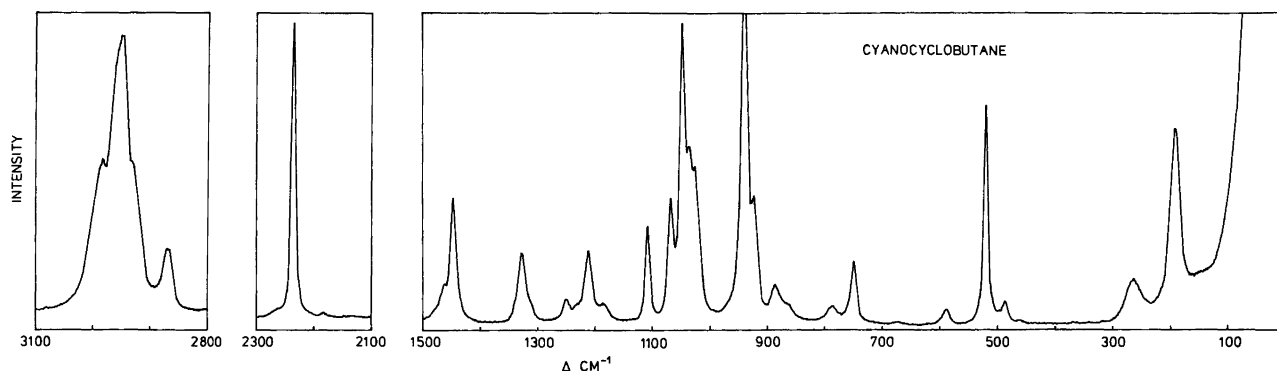


Fig. 4. Raman spectrum of CYCB as a liquid at 259 K.

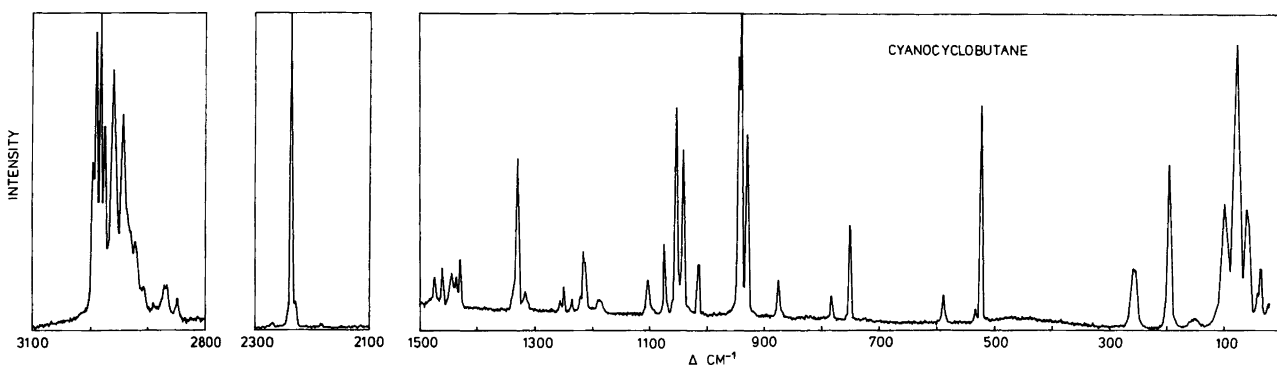


Fig. 5. Raman spectrum of CYCB as a crystalline solid (crystal III, see text) formed by cooling a liquid to 173 K.

Table 1. Infrared and Raman spectral data for cyanocyclobutane.<sup>a</sup>

| Infrared                          |                                     |   |                              |   |                              | Raman           |                              | Assign.                                 |
|-----------------------------------|-------------------------------------|---|------------------------------|---|------------------------------|-----------------|------------------------------|---|
| Vapour                            | Ar-matrix<br>14 K                   | N <sub>2</sub> -matrix<br>14 K              | Liquid                       | Solid<br>crystal<br>90 K                              | High-<br>pressure<br>crystal | Liquid<br>200 K | Solid<br>crystal<br>90 K     |   |
| 3010 }<br>3004 } vs, A<br>2998 }  | 3001 vs                             | 3007 vs<br>3001 m, sh                       | 2996 vs                      | 2996 vs   | 3047 w                       | 2996 m, sh      | 2997 w, sh                   | $\nu_1$                                 |
| 2994 }<br>2989 } s, A<br>2983 }   | 2993 m                              | 2995 m                                      | 2986 m, sh                   | 2988 s  | 3015 m                       | 2984 s, P       | 2990 ms                      | $\nu_2$                                 |
| 2980 }<br>2975c } m, B<br>2970 }  | 2988 w, sh                          | 2990 w, sh                                  | 2963 w, sh                   | 2981 s  | 2995 w, sh                   | 2960 vw, D?     | 2982 ms                      | $\nu_{21}$                              |
| 2968 }<br>2961 } m, A<br>2958 }   | 2966 w, sh<br>2961 vs<br>2955 w, sh | 2964 s                                      | 2954 vs                      | 2956 ms   | 2974 }<br>2969 }             | 2950 vs, P      | 2959 ms                      | $\nu_3$                                 |
| 2946 }<br>2942 } w, A<br>2936 }   | 2936 vw                             | 2940 vw                                     | 2936 w, sh                   | 2942 m  |                              | 2934 w, P       | 2942 ms                      | $\nu_4$                                 |
| 2930 }<br>2923 } vw, A?<br>2916 } | 2928 vw                             | 2933 vw                                     | 2925 w, sh                   | 2925 mw   | 2925 w, sh                   |                 | 2921 w                       | $\nu_7 + \nu_8$                         |
| 2915 vw<br>2902 vvw               | 2900 vvw                            | 2904 vvw                                    | 2895 vw                      | 2910 vw<br>2896 vw<br>2882 vw                         |                              |                 | 2906 vw<br>2890 vvw          | $2 \times \nu_8$<br>$2 \times \nu_{23}$ |
| 2897 }<br>2889 } w, A<br>2881 }   | 2883 w, sh<br>2877 m                | 2884 w, sh<br>2879 m                        | 2873 m                       | 2871w }<br>2871m }                                    | 2872 m                       | 2872 ms, P      | 2869 ms                      | $\nu_5$                                 |
| 2871 }<br>2861 }                  | 2870 vvw                            | 2870 vvw                                    |                              | 2847 mw   |                              |                 | 2848 w, sh                   | $\nu_{22}?$                             |
| 2280 vw                           | 2273 w<br>2268 vw                   | 2272 vw                                     | 2260 w, sh                   | 2268 w<br>2254 vvw                                    |                              | 2260 vw         | 2256 vw                      |   |
| 2251 }<br>2240 } m, A<br>2229 }   | 2245 vs<br>2242 m, sh<br>2229 vw    | 2241 vs<br>2227 w                           | 2237 vs                      | 2235 vs<br>2227 s, sh<br>2209 vvw                     |                              | 2239 vs, P      | 2235 s                       | $\nu_6$                                 |
| 1482 }<br>1478 } w, A<br>1474 }   | 1476 vw                             | 1480 vw                                     | 1475 vvw                     | 1470 mw   | 1472vvw                      | 1478 vw, sh     | 1473 vw                      | $\nu_7$                                 |
| 1460 }<br>1453 } m, A<br>1445 }   | 1464 w<br>1460 w                    | 1463 w                                      | 1460 w, sh                   | 1463 vw, sh<br>1453 ms                                | 1450 m                       | 1462 w, P?      | 1460 w                       | $\nu_8$                                 |
| 1440 }<br>1435c } w, B<br>1431 }  | 1449 ms<br>1444 m<br>1436 w, sh     | 1451 ms<br>1445 m<br>1436 vw, sh<br>1378 vw | 1445 s<br>1383 vw<br>1372 vw | 1440 m<br>1432 ms<br>1425 vw, sh<br>1368 w<br>1362 vw | 1438 vs                      | 1446 m, P       | 1445 w<br>1437 vvw<br>1431 w | $\nu_{23}$                              |
| 1334 }<br>1327 } w, A<br>1323 }   | 1335 w<br>1329 w                    | 1335 w<br>1329 w                            | 1327 w                       | 1328 w  | 1328 w                       | 1327 m, P       | 1330 m                       | $\nu_9$                                 |
| ~1270 vw                          | 1281 w<br>1277 w<br>1251 w, sh      | 1313 vw<br>1282 vw, sh<br>1279 w            | 1311 vvw                     | 1315 vvw  | 1318 vw                      | 1320 vw, D?     | 1317 vw                      |   |
| ~1250 w                           | 1249 s<br>1247 s<br>1231 vw         | 1250 s                                      | 1247 s                       | 1246 s  | 1247 vs                      | 1250 w, P?      | 1250 w                       | $\nu_{10}$                              |
|                                   | 1219 m                              | 1233 w<br>1222 vw, sh<br>1220 w, sh         |                              | 1234 m<br>1222 ms<br>1219 mw                          |                              | 1232 vw, D?     | 1235 vw<br>1220 vw, sh       | $\nu_{25}$<br>$\nu_{26}$                |

contd

Table 1. (contd)

| Infrared                       |           |                        |            |               |                       | Raman                 |               | Assign.               |
|--------------------------------|-----------|------------------------|------------|---------------|-----------------------|-----------------------|---------------|-----------------------|
| Vapour                         | Ar-matrix | N <sub>2</sub> -matrix | Liquid     | Solid crystal | High-pressure crystal | Liquid                | Solid crystal |                       |
|                                | 14 K      | 14 K                   |            | 90 K          |                       | 200 K                 | 90 K          |                       |
| ~1219 vw                       |           |                        | 1210 m     |               | 1213 vw               | 1213 m, P             |               |                       |
|                                | 1215 w    | 1217 m                 |            | 1215 m        |                       |                       | 1216 mw       | $\nu_{11}$            |
|                                | 1213 w    | 1215 m                 |            | 1211 vw       |                       |                       | 1213 w, sh    |                       |
|                                | 1186 vw   | 1188 vw                | 1182 vw    | 1192 m        | 1200 s                | 1185 vw, D            | 1189 vw       | $\nu_{27}$            |
|                                | 1177 w    | 1179 w                 |            | 1183 vvw      |                       |                       |               |                       |
|                                | 1124 vvw  | 1126 vvw               |            |               |                       |                       |               |                       |
| 1117 }<br>1109 }w, A<br>1101 } | 1109 m    | 1111 m                 | 1106 s     | 1097 ms       | 1101 ms               | 1108 m, P             | 1103 w        | $\nu_{12}$            |
|                                | 1097 vvw  | 1097 vvw               |            |               |                       |                       |               |                       |
|                                | 1070 vw   | 1071 w                 | 1067 vw    | 1074 m        | 1087 mw               | 1070 m, P             | 1074 mw       | $\nu_{20} + \nu_{30}$ |
|                                | 1067 vw   | 1068 vw                |            |               |                       |                       |               | $\nu_{15} + \nu_{33}$ |
|                                | 1050 vw   | 1050 w                 | 1049 vw    | 1053 m        | *                     | 1049 vs, P            | 1054 s        | $\nu_{13}$            |
|                                | 1041 w    | 1045 vw                |            |               |                       |                       |               |                       |
|                                | 1029 w    | 1033 w                 | 1035 w     | 1040 m        | *                     | 1039 ms, P?           | 1042 ms       | $2 \times \nu_{18}$   |
|                                |           |                        |            |               | 1045 w, bd            | 1025 mw, P $\uparrow$ | *             | $\nu'_{13}$           |
|                                | 1014 vvw? | 1015 vw                | 1017 vw    | 1017 m        | 1024 mw               | 1016 vw, D            | 1015 mw       | $\nu_{28}$            |
|                                | 942 m     | 942 m                  |            | 947 w         | 953 m                 |                       | 946 s, sh     | $\nu_{29}$            |
| ~940 vw                        |           |                        | 938 m      |               |                       | 937 vs, P             |               |                       |
|                                | 939 m     | 936 m                  |            | 942 ms        | 941 m                 |                       | 942 vs        | $\nu_{14}$            |
| 927 }<br>922 }w, B<br>916 }    | 917 m     | 920 m                  | 921 s      | 924 ms        | 932 s                 | 923 m, D              | 930 ms        | $\nu_{30}$            |
| ~888 vvw?                      | 891 w     | 892 w, sh              |            | 880 ms        | *                     | 885 w, P              | 876 w         | $\nu_{15}$            |
|                                | 882 w     | 889 mw                 | 887 w      | 880 ms        | *                     |                       |               |                       |
|                                |           |                        | 860 vvw?   | *             | 850 mw                | 865 vw, P $\uparrow$  | *             | $\nu'_{15}$           |
|                                | 813 vw    | 815 vw                 | 815 vw     | 816 vw        |                       |                       |               |                       |
|                                |           | 789 vw, sh             |            |               |                       |                       |               |                       |
| 792 }<br>782 }w, B<br>772 }    | 783 mw    | 786 vw, sh             | 785 w      | 785 ms        | 771 ms                | 787 vw, D             | 783 vw        | $\nu_{31}$            |
|                                |           | 785 m                  |            |               |                       |                       |               |                       |
|                                | 767 vw    | 766 vw                 |            |               |                       |                       |               |                       |
| 750 }<br>743 }w, A<br>735 }    | 744 s     | 748 s                  | 747 s      | 748 s         | 733 ms, bd            | 749 m, P              | 752 mw        | $\nu_{16}$            |
|                                |           |                        |            |               |                       |                       |               |                       |
|                                |           | 721 vw                 | 720 w      | 724 w         |                       |                       | 722 vvw       | $\nu_{17} + \nu_{20}$ |
|                                |           |                        |            | 717 vw        |                       |                       |               |                       |
|                                | 709 w     | 713 w                  |            | *             | ~680 vvw?             | ~670 vw, P $\uparrow$ | *             | $\nu_{18} + \nu_{33}$ |
|                                |           | 677 vw                 | 676 w      | *             | ~620 vvw?             |                       |               | $\nu'_{17}$           |
| ~580 vw                        | 582 mw    | 586 vw, sh             | 589 m      | 588 ms        | *                     | 587 vw, P?            | 588 w         | $\nu_{17}$            |
|                                | 579 mw    | 584 m                  |            | 584 vw, sh    |                       |                       |               |                       |
|                                |           | 583 vw, sh             | 535 vw, sh | 534 w         | 542 vw                | ~530 vw, sh           | 534 vw        | $\nu_{32}$            |
| ~518 vw                        | 515 m     | 521 vw, sh             | 518 m      | 522 ms        | *                     | 521 s, P              | 525 s         | $\nu_{18}$            |
|                                |           | 517 m                  |            | 500 vw        |                       |                       |               |                       |
|                                |           |                        | 484 w      | 490 vw        |                       |                       |               |                       |
|                                | 478 vw    | 475 vw?                |            | *             | 518 m                 | 486 w, P $\uparrow$   | *             | $\nu'_{18}$           |
|                                | 356 w     |                        |            |               |                       |                       |               |                       |
|                                | 273 w     |                        | 268 vw     | 257 m         | 243 mw                | 265 mw, P?            | 259 mw        | $\nu_{19}$            |
|                                |           |                        | 190 m      | 190 m         | 215 m                 | 191 s, D?             | 197 s         | $\nu_{33}$            |
|                                |           |                        | 152 vw     | 149 m         | ~150 w                | ~150 vw               | 150 vw        | $\nu_{20}$            |
|                                |           |                        |            |               | ~130 w                |                       |               |                       |
|                                |           |                        |            | 95 m          | ~100 w                |                       | 97 ms         | l. m.                 |
|                                |           |                        |            | 84 m          | ~85 w                 |                       | 78 vs         | l. m.                 |
|                                |           |                        |            | 62 w          |                       |                       | 59 ms         | l. m.                 |

<sup>a</sup>Abbreviations: s, strong; m, medium; w, weak; v, very; sh, shoulder; c, central; bd, broad; P, polarized; D, depolarized; A, B, and C denote vapour contours; arrows ( $\uparrow$ ) in Raman spectra denote bands enhanced at higher temperatures; asterisks (\*) signify bands believed to be due to an unstable conformer.

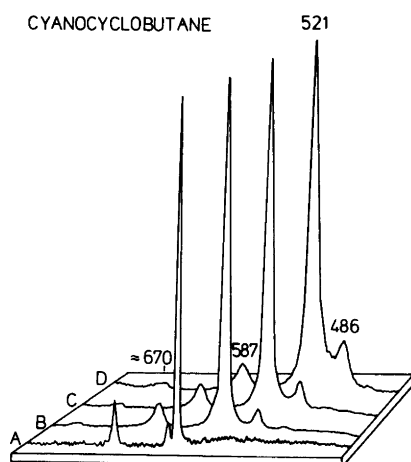


Fig. 6. Raman curves of CYCB in the region 700–400  $\text{cm}^{-1}$ ; A, crystalline solid at 173 K; B, liquid at 202 K; C, liquid at 231 K; D, liquid at 295 K.

**Matrix Spectra.** The matrix spectra were recorded in order to observe bands of the unstable conformer in the matrices. With the hot-nozzle technique (covering the range 313–900 K) the equilibrium should be highly displaced and the unstable conformer (axial) bands strongly enhanced, making a  $\Delta H^\circ$  determination of the vapour equilibrium feasible.

However, as is apparent from Fig. 1 we found no trace of the axial conformer bands in any of the matrix spectra, regardless of the nozzle temperature. Thus, at a temperature of ca. 17 K maintained at the CsI window during deposition, barriers lower than 5  $\text{kJ mol}^{-1}$  will not prevent the molecules, originally in the unstable conformation (axial), from converting to the more stable (equatorial) conformation at an appreciable rate. This result is in agreement with the recent results from microwave spectro-

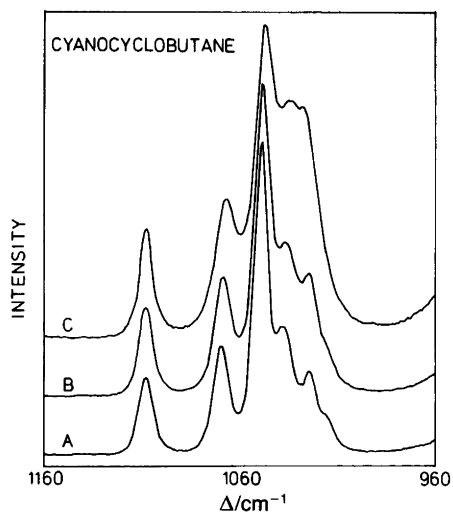


Fig. 7. Raman curves of CYCB as a liquid in the 1160–960  $\text{cm}^{-1}$  range; A, 202 K; B, 231 K; C, 295 K.

scopy<sup>8,9</sup> giving 310  $\text{cm}^{-1}$  (3.67  $\text{kJ mol}^{-1}$ ) as the barrier height for CYCB. It was reported recently<sup>2</sup> that chloro- and bromocyclobutane also have barriers lower than 5  $\text{kJ mol}^{-1}$ , as seen from the matrix spectra. The same was true for the dihalogenated compound 1-chloro-1-fluorocyclobutane,<sup>10</sup> whereas the polyhalogenated analogues 1-chloro-1,2,2-trifluoro- and 1,1,2-trichloro-2,3,3-trifluorocyclobutane<sup>10</sup> have barriers close to 7  $\text{kJ mol}^{-1}$ .

The spectra of CYCB in the nitrogen and argon matrices were quite similar, although more bands were split in the argon matrix. These splittings were mostly caused by multiple trapping sites, since they disappeared after annealing.

No evidence for decomposition in the matrices was seen, even at 900 K. From the results of a study of the thermal decomposition of cyanocyclobutane between 730 and 780 K<sup>11</sup> we were able to estimate a reaction rate at 900 K. This rate constant is such that for 1% decomposition to occur, the sample would need to be at that temperature for  $3 \times 10^{-4}$  seconds, which is slightly more than, but of the same order of magnitude as, the length of time each molecule spends in the hot nozzle.

**Low temperature crystal spectra.** When the vapour of CYCB was shock frozen on a CsI window (IR) or on a copper block (Raman) at ca. 85 K an amorphous solid was obtained. The resulting spectrum had broad bands and was rather similar to the spectrum of the liquid (with some differences, see above). The sample was annealed by heating to ca. 135 K and then recooled to 85 K, and significant changes in the spectra took place, suggesting that a crystalline sample was obtained (crystal I). Annealing at 140 K and recoiling to 85 K gave another solid spectrum with sharp peaks and considerable crystal splitting (crystal II). Finally, when the sample was annealed at 185 K (fairly close to the melting point) before cooling to 85 K, a third crystalline spectrum appeared which was quite different from the two others (crystal III).

Thus, CYCB has various crystalline phases which can be obtained by annealing the amorphous solid. Apparently, phase III is thermodynamically stable, while I and II are metastable phases which cannot be formed by cooling phase III. Independent Raman spectra of crystalline CYCB obtained by cooling a liquid below the melting point invariably gave spectra of phase III. It is not quite clear whether phase I is a real crystalline phase or a partly amorphous, partly crystalline phase.

All the low-temperature crystalline phases consist of molecules which are in the more stable equatorial conformation. The four bands at 1025, 865, 676 and 486  $\text{cm}^{-1}$ , attributed to the axial conformer on the basis of the temperature variation, disappear completely in the crystal spectra. It is also significant that a thermodynamic equilibrium is maintained in the amorphous solid at 85 K, giving a negligible concentration of the axial conformer at this temperature. For the sake of brevity, only the crystal III data are given in Figs. 2 (IR) and 5 (Raman) and in Table 1.

*High pressure crystal.* As is apparent from Fig. 3 and from Table 1, the IR spectrum of the high-pressure crystal of CYCB was quite different from that of the liquid. Moreover, the high-pressure crystal spectrum differs dramatically from the spectrum of the low-temperature crystals. This observation is in complete variance with the results for chloro- and bromocyclobutane,<sup>2</sup> for which the bands for the high-pressure crystal were merely shifted a few wavenumbers upwards relative to the low-temperature crystal. It thus appears that the forms present in the two crystals are different. Inasmuch as many of the bands found in the high-pressure crystal spectrum have no counterparts in the infrared spectrum of the liquid, we initially hesitated before asserting that the form present in the high pressure crystal is the axial conformer.

We were concerned first that the compound might in some way have undergone a reaction at high pressure, but the release of pressure on the enclosed crystalline sample resulted in the return of the spectrum to that which we had seen earlier for the liquid.

The pressure was reduced so as to achieve partial melting, with only one or a few crystallites remaining. After subsequent pressure increase, one or a few single crystals were formed. By repeating this procedure, a single crystal of CYCB was formed. The IR spectrum was not significantly different from the polycrystalline spectrum except that a very weak band at  $1362\text{ cm}^{-1}$  present in the spectrum of the polycrystalline sample vanished in the single crystal spectrum.

Attempts were made to study the conformational equilibrium as a function of pressure. Thus, we tried to increase the pressure in small increments prior to crystallization. Secondly, a 20% solution of CYCB in  $\text{CS}_2$  was pressurized. If the axial conformer of CYCB had a smaller molar volume than the equatorial, which is the case for a variety of substituted cyclohexanes,<sup>12,13</sup> the equilibrium should be shifted towards the axial conformer with increasing pressure. However, no definite effect could be observed in which the axial bands ( $1025, 865, 676$  and  $486\text{ cm}^{-1}$ ) were enhanced under pressure.

Three alternatives seem possible to interpret the spectra of the high-pressure crystal:

- (1) it contains molecules in the axial conformer;
- (2) it contains molecules in the equatorial conformer, apparently of a different crystal than any of the three low-temperature crystals I, II and III;
- (3) it contains the equatorial (or possibly the axial) conformer, but the cyclobutane ring is distorted (flattened) under pressure.

The alternative (3) is related to the observations of Lewis and Whalley,<sup>14</sup> in which they claim a flattening of the trithiane ring with pressure, producing shifts and intensity variations of the bands. However, no distinct band displacements with further pressure increase within the high-

pressure crystalline phase were observed, making this alternative unlikely.

Both the alternatives (1) and (2) were carefully checked by correlating the IR and Raman bands from the various phases. For both alternatives, certain unreasonably large IR spectral shifts from the liquid to the high-pressure crystal and from the low-temperature to the high-pressure crystals had to be accepted. These shifts were larger than we have encountered in the long series of high-pressure crystals of conformational mixtures which have been studied in this laboratory.<sup>13</sup> In alternative (2) it was necessary to correlate the  $880\text{ cm}^{-1}$  band of the low-temperature crystal with the band at  $850\text{ cm}^{-1}$  of the high-pressure crystal. A negative shift of  $30\text{ cm}^{-1}$  seems completely unacceptable, since the bands are generally displaced to higher wavenumbers with increasing pressure. Also, it is easier to accept large shifts for alternative (1) than for (2). Apart from the observed axial bands ( $1025, 865, 676$  and  $486\text{ cm}^{-1}$ ) and their assumed equatorial analogues ( $1049, 887, 589$  and  $518\text{ cm}^{-1}$ ) (liquid), the majority of liquid bands in Table 1 will be common to the equatorial and the axial conformers. The large negative shifts between IR bands of the low-temperature and high-pressure crystals ( $14\text{ cm}^{-1}$  of  $\nu_{31}$  and  $15\text{ cm}^{-1}$  of  $\nu_{16}$ ) are more easily accepted when they are due to different conformers.

From a variety of arguments we have tentatively attributed the high-pressure crystal bands to molecules in the axial conformation [alternative (1)], and the assignments of Table 1 are based upon this assumption.

*Conformational behaviour.* The enthalpy difference  $\Delta H^0$  (axial–equatorial) for CYCB ( $4.8 \pm 0.4\text{ kJ mol}^{-1}$ ) can be compared with the results for chlorocyclobutane<sup>2</sup> [ $5.2 \pm 1.9$  (vapour),  $5.7 \pm 0.7\text{ kJ mol}^{-1}$  (liquid)], bromocyclobutane<sup>2</sup> [ $8.2 \pm 1.2$  (vapour),  $9.0 \pm 0.5\text{ kJ mol}^{-1}$  (liquid)] and methylcyclobutane<sup>3</sup> [ $3.5 \pm 0.9$  (vapour),  $4.2 \pm 2.1\text{ kJ mol}^{-1}$  (liquid)]. Similar  $\Delta H^0$  values are to our knowledge not shown for the monosubstituted cyclohexanes, but some  $-\Delta G^0$  (axial–equatorial) at coalescence temperature (around  $190\text{ K}$  in  $\text{CS}_2$  solution) are reported,<sup>15</sup> being  $1.00, 2.21$  and  $1.99\text{ kJ mol}^{-1}$  for cyano-, chloro- and bromocyclohexane. Although these data cannot be directly compared, it is a fact that the conformational equilibria shifted more towards the equatorial conformer in cyclobutanes, while the barriers to ring conversion are much higher in the cyclohexanes (ca.  $40\text{ kJ mol}^{-1}$ ). In cyclohexanes the conformational equilibria are highly dependent upon the 1,3-parallel diaxial repulsion between the substituent X and a hydrogen. Therefore, the narrow pivot-shaped  $-\text{C}\equiv\text{N}$  group gives a lower 1,3 diaxial repulsion and an equilibrium which is shifted more towards the axial conformer than for the halocyclohexanes. The smaller puckering angle and divergent 1,3 diaxial bonds in cyclobutanes<sup>16</sup> increase the non-bonded  $\text{X}\cdots\text{H}$  distance in the 1,3 diaxial position, and other terms such as the 1,2-geminal  $\text{X}\cdots\text{H}$  repulsion as well as dipole interactions contribute to the conformational en-

Table 2. Observed and calculated frequencies for cyanocyclobutane.

| $\nu_i$ | Equatorial        |       | PED <sup>b</sup>  | Axial |       | $\nu(\text{eq}) - \nu(\text{ax})$ |       |
|---------|-------------------|-------|---|-------|-------|-----------------------------------|-------|
|         | Obs. <sup>a</sup> | Calc. |   | Obs.  | Calc. | Obs.                              | Calc. |
| 9.      | 1327              | 1336  | 36 $\alpha$ CH $\delta$ , 15CC(N)st, 14 $\beta$ CH <sub>2</sub> wa                    |       | 1346  |                                   | -10   |
| 10.     | 1250              | 1276  | 52 $\beta$ CH <sub>2</sub> wa, 16 $\beta$ CH <sub>2</sub> tw, 16 ring st              |       | 1286  |                                   | -10   |
| 11.     | 1216              | 1223  | 56 $\beta$ CH <sub>2</sub> tw, 12 $\gamma$ CH <sub>2</sub> ro                         |       | 1219  |                                   | 4     |
| 12.     | 1109              | 1131  | 42 ring st (breath), 21CC(N)st  |       | 1071  |                                   | 60    |
| 13.     | 1049              | 1045  | 48 $\alpha$ CH $\delta$ , 6 $\beta$ CH <sub>2</sub> ro, 4 $\gamma$ CH <sub>2</sub> ro | 1025  | 1038  | 20                                | 7     |
| 14.     | 942               | 969   | 38 ring st, 14 $\beta$ CH <sub>2</sub> ro, 9 ring $\delta$                            |       | 900   |                                   | 69    |
| 15.     | 888               | 886   | 34 ring st, 28 ring $\delta$ , 12 $\gamma$ CH <sub>2</sub> ro                         | 865   | 865   | 23                                | 21    |
| 16.     | 743               | 758   | 44 $\gamma$ CH <sub>2</sub> ro, 24 ring st, 16 $\beta$ CH <sub>2</sub> tw             |       | 816   |                                   | -58   |
| 17.     | 580               | 586   | 47 ring $\delta$ , 34 $\beta$ CH <sub>2</sub> ro, 14 $\gamma$ CH <sub>2</sub> ro      | 670   | 650   | -90                               | -64   |
| 18.     | 518               | 508   | 37CC(N)st, 30CCC(N) $\delta$ , 10 ring st   | 486   | 499   | 32                                | 9     |
| 19.     | 265               | 251   | 52CCN $\delta$ , 42 ring puck.  |       | 257   |                                   | -6    |
| 20.     | 150               | 155   | 76 ring puck., 25CCN $\delta$ , 24 $\beta$ , $\lambda$ CH <sub>2</sub> ro             |       | 142   |                                   | 13    |
| 24.     | 1279              | 1262  | 64 $\gamma$ CH <sub>2</sub> wa, 18 $\beta$ CH <sub>2</sub> wa, 14 ring st             |       | 1266  |                                   | -4    |
| 25.     | 1232              | 1241  | 34 $\beta$ CH <sub>2</sub> wa, 28 $\alpha$ CH $\delta$ , 18 ring st                   |       | 1258  |                                   | -17   |
| 26.     | 1220              | 1214  | 50 $\gamma$ CH <sub>2</sub> tw, 24 $\beta$ CH <sub>2</sub> tw                         |       | 1215  |                                   | -1    |
| 27.     | 1185              | 1187  | 40 $\beta$ CH <sub>2</sub> wa, 36 ring st, 21 $\gamma$ CH <sub>2</sub> wa             |       | 1186  |                                   | 1     |
| 28.     | 1016              | 1034  | 72 $\beta$ CH <sub>2</sub> tw, 19 $\gamma$ CH <sub>2</sub> tw                         |       | 1036  |                                   | -2    |
| 29.     | 946               | 930   | 60 ring st  |       | 957   |                                   | 27    |
| 30.     | 922               | 919   | 42 ring st, 40 $\alpha$ CH $\delta$   |       | 902   |                                   | 17    |
| 31.     | 782               | 772   | 88 $\beta$ CH <sub>2</sub> ro, 16 $\gamma$ CH <sub>2</sub> tw                         |       | 760   |                                   | 12    |
| 32.     | 530               | 525   | 51CCC(N) $\delta$ , 24 ring st, 21CCN $\delta$  |       | 523   |                                   | 2     |
| 33.     | 191               | 196   | 76CCN $\delta$ , 20CCC(N) $\delta$  |       | 201   |                                   | -5    |

<sup>a</sup>IR vapour or Raman liquid and solid phase values. Fundamentals above 1400 cm<sup>-1</sup> have been omitted. <sup>b</sup>Potential energy distribution defined as  $X_{ik} = 100F_{ik}L_{ik}^2/\gamma_k$ ; st, stretch;  $\delta$ , deformation; ro, rock.; wa, wag.; tw, twist.; sc, scissor.;  $\alpha$ ,  $\beta$ ,  $\gamma$  denote carbon positions in the ring; adjusted force constants: CC(N)st 5.116 mdyn/A, CNst 17.23 mdyn/A, CCC(N) $\delta$  in-plane 2.150 mdyn A/rad<sup>2</sup>, CCH $\delta$  in-plane 0.936 mdyn A/rad<sup>2</sup>, CCC(N) $\delta$  out-of-plane 1.594 mdyn A/rad<sup>2</sup>, CCH $\delta$  out-of-plane 0.608 mdyn A/rad<sup>2</sup>, CCN $\delta$  0.227 mdyn A/rad<sup>2</sup>, ring puckering 0.211 mdyn A/rad<sup>2</sup>, CC(N)st/CCH $\delta$  in-plane -0.685 mdyn/rad.

ergies. For these reasons the analogies between the conformational energies of substituted cyclobutanes and cyclohexanes under pressure should not be carried too far.

In monohalo- and *trans*-1,4-dihalocyclohexanes the conformational equilibria are shifted towards the axial or diaxial conformer with pressure,<sup>12,13</sup> this obviously being caused by a small molar volume of the axial conformer. Cyano-, isocyano-<sup>17</sup> and isocyanatocyclohexane<sup>18</sup> all crystallize in the axial conformation under pressure, whereas ethynyl-,<sup>19</sup> isothiocyanato<sup>18</sup> and *trans*-1,4-dicyanocyclohexane<sup>20</sup> crystallize in the equatorial (or diequatorial) conformation at low temperature as well as under high pressure. However, when the axial or diaxial conformer crystallizes at high pressure this conformer is already present in substantial amounts at atmospheric pressure. In the present case, the axial conformer is present in less than 10% abundance in the liquid at ambient temperature. Therefore, there must be a substantial difference in the molar volumes of the two conformers of CNCB and a very favourable enthalpy of crystallization of the axial conformer under pressure.

**Spectral assignments.** The spectral assignments for CNCB are listed in Table 1, and the fundamentals below 1400 cm<sup>-1</sup> are given in Table 2 together with the results of the force constant calculations. Apart from the three modes associated with the C-C $\equiv$ N group (C $\equiv$ N stretch at 2237 cm<sup>-1</sup>

and in-plane and out-of-plane CCN bending at 265 and 191 cm<sup>-1</sup>) the IR and Raman spectra of CNCB are very similar to those of chloro- and bromocyclobutane,<sup>2</sup> and no lengthy discussion seems necessary. In the region 1300–1150 cm<sup>-1</sup> seven prominent IR and Raman bands for chloro- and bromocyclobutane (in the cooled liquids) were considered as fundamentals;<sup>2</sup> a few additional bands were observed for CNCB in this region (ascribed as combination bands or overtones) and seven equatorial bands ( $\nu_9 - \nu_{11}$  and  $\nu_{24} - \nu_{27}$ ) were assigned as fundamentals.

The assignments of IR and Raman bands as being of purely axial origin (1025, 865, 670 and 486 cm<sup>-1</sup>), as well as that of their equatorial counterparts (1049, 888, 580 and 518 cm<sup>-1</sup>), were based upon their disappearance in the low-temperature and high-pressure crystal spectra and on the intensity variations with temperature (see above). For chlorocyclobutane we observed five, and for bromocyclobutane four corresponding band pairs.<sup>2</sup> Presumably, the remaining axial conformer bands in CYCB, as well as in the two halogenated cyclobutanes, are covered by the much more intense equatorial bands. It is significant that the observed axial bands in the three monosubstituted cyclobutane are all situated in the region 1100–350 cm<sup>-1</sup> and involve ring stretch, CH bend, CH<sub>2</sub> rock, C-halogen<sup>2</sup> stretch and C-C(N) stretch. These bands should clearly be intense and be shifted away from the equatorial band in



order to be observed. The agreement between the observed and calculated shifts,  $\nu(\text{eq})-\nu(\text{ax})$ , is not satisfactory for CYCB (Table 2), but the agreement is somewhat better for chloro- and bromocyclobutane.<sup>2</sup>

The force-field for CYCB was derived by transferring force constants obtained for chloro and bromocyclobutane,<sup>2</sup> whereas the stretching and bending constants for the C-C≡N moiety were taken from work on cyanocyclohexane.<sup>17</sup> When the spectral data for additional di- and polyhalogenated cyclobutanes, presently being studied in our laboratory, have been analysed, we plan to derive an improved force field for the cyclobutanes.

**Acknowledgements.** The authors are grateful to Anne Horn and Gunnar Isaksen for valuable assistance. Financial support was provided by the Research Corporation, the Norwegian Marshall Fund, NAVF and NTNF.

## References

- Allen, F. H. *Acta Crystallogr., Sect. B* **40** (1984) 64.
- Gatjal, A., Klæboe, P., Nielsen, C. J., Powell, D. L., Sülzle, D. and Kondow, A. J. *J. Raman Spectrosc. In press.*
- Durig, J. R., Geyer, T. J., Little, T. S. and Kalasinsky, V. F. *J. Chem. Phys.* **86** (1987) 545; Kalasinsky, V. F., Harris, W. C., Holtzclaw, P. W., Little, T. S., Geyer, T. J. and Durig, J. R. *J. Raman Spectrosc.* **18** (1987) 581.
- Reitz, A. W. and Skrabal, R. *Monatsh.* **70** (1937) 398.
- Blackwell, C. S., Carreira, L. A., Durig, J. R., Karriker, J. M. and Lord, R. C. *J. Chem. Phys.* **56** (1972) 1706.
- Durig, J. R., Carreira, L. A. and Lafferty, W. J. *J. Mol. Spectrosc.* **46** (1973) 187.
- Fong, M. Y. and Harmony, M. D. *J. Chem. Phys.* **58** (1973) 4260.
- Caminati, W., Velino, B., Dakkouri, M., Schäfer, L., Siam, K. and Ewbank, J. D. *J. Mol. Spectrosc.* **123** (1987) 469.
- Caminati, W., Velino, B. and Valle, R. G. D. *J. Mol. Spectrosc.* **129** (1988) 284.
- Powell, D. L., Gatjal, A., Klæboe, P., Nielsen, C. J. and Kondow, A. J. *J. Mol. Struct.* **173** (1988) 389.
- Sarner, S. F., Gale, D. M., Hall, H. K. and Richmond, A. B. *J. Phys. Chem.* **76** (1972) 2817.
- Christian, S. D., Grundnes, J. and Klæboe, P. *J. Am. Chem. Soc.* **97** (1975) 3864.
- Klæboe, P. *Z. Chem.* **21** (1981) 381.
- Lewis, G. J. and Whalley, E. *J. Chem. Phys.* **68** (1978) 1119.
- Jensen, F. R., Bushweller, C. H. and Beck, B. H. *J. Am. Chem. Soc.* **91** (1969) 344.
- Jonvik, T. *J. Mol. Struct.* **172** (1988) 213; Jonvik, T. *J. Mol. Struct. In press.*
- Woldbaek, T., Berkessel, A., Horn, A. and Klæboe, P. *Acta Chem. Scand., Ser. A* **36** (1982) 719.
- Sjøgren, C. E. and Klæboe, P. *J. Mol. Struct.* **100** (1983) 433.
- Woldbaek, T., Nielsen, C. J. and Klæboe, P. *Spectrochim. Acta, Part A* **41** (1985) 43.
- Ellestad, O. H., Klæboe, P. and Woldbaek, T. *J. Mol. Struct.* **95** (1982) 117.

Received October 27, 1988.